Determination of the S_{18} astrophysical factor for $^8B(p,\gamma)^9C$ from the breakup of ^9C at intermediate energies

L. Trache,[1] F. Carstoiu,[2,3] A. M. Mukhamedzhanov,[1] and R. E. Tribble[1]
[1]*Cyclotron Institute, Texas A&M University, College Station, Texas 77843-3366*
[2]*Institute of Physics and Nuclear Engineering Horia Hulubei, Bucharest, Romania*
[3]*Laboratoire de Physique Corpusculaire, F-14050 Caen Cedex, France*
(Received 13 June 2002; published 11 September 2002)

We have used existing data on the one-proton-removal cross section of ^9C at 285 MeV/nucleon and Glauber model calculations to extract the asymptotic normalization coefficient for the wave function of the last proton in the ground state of ^9C. The calculations are done first using folded potentials starting from two different effective nucleon-nucleon interactions and second in the optical limit using three nucleon-nucleon interactions, and the results are found to be consistent, with no new parameters adjusted. We find $C^2(p_{3/2})+C^2(p_{1/2}) = 1.22\pm0.13$ fm^{-1}. From this result we obtain the astrophysical factor for the proton radiative capture reaction $^8B(p,\gamma)^9C$ as $S_{18}(0)=46\pm6$ eV b. The calculated energy dependence of the astrophysical S factor for the energy region $E_{c.m.}=0-0.8$ MeV and the reaction rates for $T_9=0-1$ are included.

DOI: 10.1103/PhysRevC.66.035801 PACS number(s): 25.60.−t, 26.30.+k, 25.60.Dz, 27.20.+n

I. INTRODUCTION

Radiative capture reactions are of crucial importance in nuclear astrophysics. The capture of charged particles on nuclei, in particular of protons in basic processes like hydrogen burning in various stellar environments, is very much hindered by the Coulomb repulsion. This leads to very small cross sections and consequently to the well known experimental problems associated with direct determination of astrophysical S factors at very low energies [1]. Moreover, with the large number of reaction chains found to be of importance in nucleosynthesis calculations for different static and explosive burning scenarios [2–4], more data involving the capture on unstable nuclei becomes necessary. In many instances direct measurements involving unstable nuclei are very difficult or even impossible and indirect methods must be used.

It has been known for a long time that transfer reactions can be used as indirect methods for nuclear astrophysics (see, e.g., Refs. [5,1] and references therein) and various techniques have been used since. A few years ago another indirect approach based on measurements of peripheral transfer reactions was proposed [6,7], and was subsequently used to determine the astrophysical factor $S_{17}(0)$ for the reaction $^7Be(p,\gamma)^8B$ using (^7Be,^8B) transfer reactions. The method that is based on the observation that radiative capture of protons is a very peripheral process at astrophysical energies, involves the extraction of nuclear quantities called asymptotic normalization coefficients (ANC's) from proton transfer reactions and these ANCs are then used to determine the astrophysical cross sections. The method works if the transfer reactions that have much higher cross sections than the capture reactions, are also peripheral. Using secondary beams available today, such experiments can be done in a matter of days [8–12]. More recently we have shown [13] that one-nucleon-removal reactions offer an alternative and complementary technique for extracting ANCs that is particularly well adapted to rare isotopes produced using fragmentation. In the breakup of loosely bound nuclei at intermediate energies, the requirement of core survival in the final channel automatically selects core-target interactions that are highly peripheral, with the result that the wave function of the removed nucleon is probed at and beyond the core's nuclear surface. This is then very similar to the low-energy light ion transfer reactions, where the short mean free path of the ions in the optical potential leads to surface localization. In Ref. [13] ^8B breakup data at energies between 30 and 300 MeV/nucleon on a variety of targets were compared with calculations done using a Glauber model [14] to extract the same ANC as that obtained from transfer reactions at about 12 MeV/nucleon. We suggested that such experiments have the additional advantage of using beams of lesser quality, at higher energies, and therefore can be applied to nuclei farther away from the stability.

Here we use a similar approach to analyze the breakup of ^9C. Existing cross section data for the one-proton-removal reaction with ^9C at 285 MeV/nucleon on four targets [15] are used to extract the ANC for the virtual process $^9C\rightarrow{}^8B+p$. The breakup cross sections are calculated with a Glauber type model, first using the potential approach described in Ref. [13] now with two types of effective interactions, and then using a Glauber model in the optical limit, with three different prescriptions for the elementary nucleon-nucleon (*NN*) scattering amplitudes. Good consistency is obtained between the different approaches. The value of the ANC is then used to determine the astrophysical factor S_{18} for the proton radiative capture reaction $^8B(p,\gamma)^9C$ in the energy range $E_{c.m.}=0-0.8$ MeV and the reaction rate in stellar environments is obtained for the temperature range $T_9=0-1$. The ANC extracted here agrees with that obtained recently from a transfer reaction $d(^8B,^9C)n$ on a deuteron target at 14.4 MeV/nucleon [11], but our result has a smaller uncertainty.

II. THE BREAKUP OF ^9C

Much effort has been devoted in recent years to the study of exotic nuclei. In particular, it has been shown that one-

nucleon-removal reactions with radioactive projectiles at intermediate energies can be used to study their structure [16–19]. Typically an exotic nucleus $B=(Ap)$, where B is a bound state of the core A and the nucleon p, is produced by fragmentation from a primary beam, separated and then used to bombard a secondary target. After breakup occurs, the cross section and parallel momentum distribution of the core A are measured. It has been shown that the parallel momentum distribution of the detected core A can be used to establish the orbital momentum of the relative motion of the nucleon, even disentangle contributions from different contributing orbitals, and that coincidences with gamma-rays enables one to separate the contribution of different core states into the ground state of the projectile. Typically the integrated cross sections have been used to extract absolute spectroscopic factors. However, we have shown [13,20] that the extracted spectroscopic factors depend strongly on the assumed single particle wave function (or equivalently on the geometry of the binding two-body potential that produces it), and unfortunately, for exotic nuclei these potentials are poorly known and there is not much other information to put constraints on them. We have shown that because these breakup processes are essentially peripheral, especially for loosely bound nuclei, one can obtain the ANCs, rather than the spectroscopic factors. The ANC only gives information about the asymptotic tail of the wave function for the last nucleon, but does not say anything about the behavior of the many-body wave function inside the nucleus. Fortunately, this is all we need to determine peripheral observables, chief among them the astrophysical S factor for radiative proton capture reactions. The extraction of ANC also has the advantage of not depending on the fundamental assumption about the validity of the independent particle model in the whole nucleus, but only at its surface (see Refs. [21,22] and the references therein, for a discussion on this subject), or of the clusterlike structure of some loosely bound nuclei, an important characteristic.

We apply here the method described first in Ref. [13], to analyze existing one-proton-removal cross section data for ^{9}C at 285 MeV/nucleon on four different targets (C, Al, Sn, and Pb) [15]. In these experiments a beam of radioactive ^{9}C nuclei stroke the target, and the residual ^{8}B was detected. We use the same extended Glauber model [23–25] to calculate the cross sections. The applicability of such calculations for breakup reactions was discussed before in Refs. [26,27]. In all reactions where the core survives (either proton transfer or one-proton breakup) the matrix elements for the transition $B\rightarrow A+p$ include the overlap integral $I^B_{Ap}(\vec{r})$ for the nuclei A, p, and B, obtained after integration over the internal coordinates of A for the many-body fully antisymmetric wave functions, with $\vec{r}$ the vector connecting the center of mass of nucleus A with p [28]. The ground states of the loosely bound nuclei are known to be dominated by single particle features. Outside the core both the nucleon-nucleon correlation effects and the antisymmetrization effects are small and the overlap integral behaves very much like the radial wave function for a single particle in the potential given by the core [29]

$$I^B_{Aplj}(r)\rightarrow S^{1/2}_{nlj}\varphi_{nlj}(r)\rightarrow C^B_{Aplj}\frac{W_{-\eta,l+1/2}(2\kappa r)}{r}. \quad (1)$$

Here S_{nlj} is the spectroscopic factor and, in the rightmost part of the equation, C^B_{Aplj} is the asymptotic normalization coefficient defining the amplitude of the tail of the overlap integral, W is the Whittaker function, κ is the wave number, and η is the Sommerfeld parameter for the bound state (Ap). Due to Coulomb repulsion, the radiative proton capture at stellar energies takes place at very large distances from the core, in regions where approximation (1) is very good [7], but the overlap integral there, and consequently the resulting cross sections, are very small. However, the asymptotic normalization coefficients C^B_{Aplj} can be extracted from phenomena that are peripheral, but involve regions of radii much closer to the core, and therefore have larger cross sections and are easier to measure experimentally. Another important reason for larger cross sections can be, of course, the different nature of the transition operators involved. One-proton-removal reaction from loosely bound projectiles is one such phenomenon. As an example to illustrate the above statement, for the well known reaction ^{7}Be$(p,\gamma)^8$B at solar energies ($E_{\text{c.m.}}=20$ keV) the classical turning point in the entrance channel is around $r\approx 250$ fm, but the combined effect of barrier penetration, transition operator and asymptotic behavior of the ^{8}B bound state wave function makes that regions around $r\approx 50$ fm contribute most in the radiative capture process. This means that the wave function of ^{8}B is most effectively sampled at these distances, where it is very small. Going to processes where distances $r\approx 4-5$ fm contribute most, such as in the case of breakup (Fig. 1 in Ref. [13]), one can gain five to six orders of magnitude in cross section from the magnitude of the wave function alone, as suggested qualitatively above, while the only unknown quantity is the same ANC. We treat the breakup reactions in this section using two approaches in a Glauber model.

A. Glauber model calculations with folded potentials

In the extended Glauber model used here, the center of mass of the projectile (made up of core and loosely bound proton) moves on a straight line trajectory, an approximation valid at intermediate energies. The relative motion of the outer proton about the core is described by a single particle wave function with the asymptotic behavior given by Eq. (1). They are assumed to interact separately with the target. The breakup of the projectile appears from three different processes: the proton is absorbed by the target while the remaining core is scattered and detected (stripping); both the proton and the core are scattered by nuclear interaction with the target and the core is detected (diffraction dissociation); dissociation in the Coulomb field of the target. The probability for each process depends on the impact parameter of each trajectory and on the wave function for the proton-core relative motion. The total cross section for this one-proton-removal reaction is given by the integral over all impact parameters. S-matrix elements have been calculated in the

eikonal approximation including corrections up to second order [30] to assure convergence. The *S* matrix is given in this potential approximation by

$$S(b)=e^{i\chi(b)}, \tag{2}$$

where the leading term in the eikonal expansion [30] is calculated along the trajectory

$$\chi(b)=-\frac{1}{\hbar v}\int_{-\infty}^{\infty}dzV(b,z). \tag{3}$$

The *S*-matrix elements are calculated for each trajectory, the contributions to the three terms above are evaluated and then summed incoherently as

$$\sigma_{sp}=\sigma_{str}+\sigma_{diff}+\sigma_{Coul}. \tag{4}$$

For the reaction model calculations we assume that the ground state of the projectile (J^{π}) can be approximated by a superposition of configurations of the form $[I_c^{\pi_c}\otimes nlj]^{J^{\pi}}$, where $I_c^{\pi_c}$ denote the core states and nlj are the quantum numbers for the single particle wave function $\varphi_{nlj}(r)$ in a spherical mean field potential. These single particle states are normalized to unity and have the asymptotic behavior given by Eq. (1), with the single particle asymptotic normalization coefficients b_{nlj}. When more than one configuration contributes to a given core state, then the total cross section for one-nucleon breakup is written as an incoherent superposition of single particle cross sections, weighted by the spectroscopic factors $S(c,nlj)$:

$$\sigma_{-1p}=\sum S(c,nlj)\sigma_{sp}(nlj). \tag{5}$$

For ^{9}C the last proton mainly occupies the $1p_{3/2}$ and $1p_{1/2}$ orbitals around a ^{8}B core (which only has one bound state), in unknown proportions. At large distances the two orbitals have identical radial behavior and consequently have the same single particle cross section σ_{sp} and the same single particle asymptotic normalization coefficient b_p. The one-proton-removal cross section (5) can be written as the sum of two components:

$$\begin{aligned}\sigma_{-1p}&=[S(1p_{3/2})+S(1p_{1/2})]\sigma_{sp}(1p_j)\\&=(C^2_{p_{3/2}}+C^2_{p_{1/2}})\sigma_{sp}(1p_j)/b_p^2\end{aligned} \tag{6}$$

and we can only extract the sum of the two spectroscopic factors or the sum of the two (squares of) ANCs, $C^2_{eff}=C^2_{p_{3/2}}+C^2_{p_{1/2}}$. This same sum appears in the evaluation of the astrophysical *S* factor. Here we have only considered the $1p_{3/2}$ orbital. This was taken as the solution of a radial Schrödinger equation in a Woods-Saxon potential with a geometry given by its half radius and diffuseness parameters (R,a) and a spin-orbit term with strength $V_{LS}=18.6$ MeV fm^2 [31]. The depth of the potential was adjusted to reproduce the experimental separation energy of the last proton $S_p=1.296$ MeV, for each geometry [different values of (R,a) used].

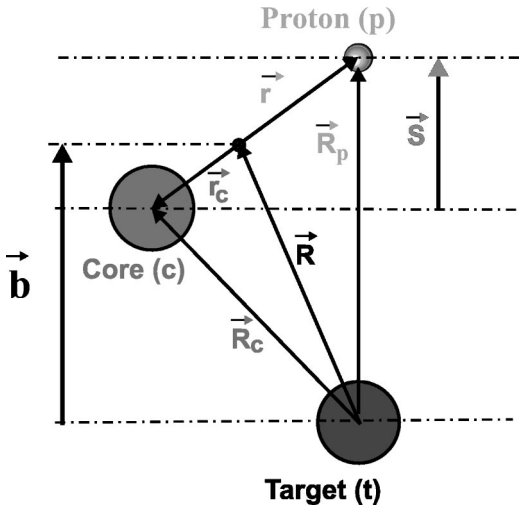

FIG. 1. The coordinate system used in the Glauber model calculations.

The coordinate system used in the Glauber calculations is shown in Fig. 1. To calculate the *S*-matrix elements we need the interaction potentials between the three participants. For the proton-target potential we have used, as we did before, the *G*-matrix effective interaction of Jeukenne, Lejeune, and Mahaux (JLM) [32], in the updated version of Ref. [33]. This interaction is complex, energy and density dependent and was adjusted for a very wide range of targets and proton energies. For the target-core potential the double folding procedure described in Ref. [34] was used, the same JLM interaction was folded with Hartree-Fock nuclear matter distributions of the core and of the target. The single particle densities were obtained in a spherical Hartree-Fock calculation using the density functional method of Beiner and Lombard [35]. The strength of the surface term in the functional method was adjusted slightly in order to reproduce the known experimental binding energy for each nucleus. This procedure, similar to those used in Refs. [36,37], leads to root-mean-square radii of the proton and mass distributions $\langle r_p^2\rangle^{1/2}=2.57$ fm and $\langle r_m^2\rangle^{1/2}=2.43$ fm, respectively, for ^{8}B, in fair agreement with our experimental determination using the ANC method [38]. The local density approximation was improved to include finite range effects by using smearing normalized Gaussian functions of ranges t_R and t_I. The resulting double folding potentials were subsequently renormalized to reproduce a variety of elastic scattering data for light nuclei. We found in Ref. [34] that at incident energies of about 10 MeV/nucleon the real part of the potential needed a smearing with a Gaussian of range $t_R=1.2$ fm and a substantial renormalization ($N_V=0.37$), while the imaginary part did not need renormalization ($N_W=1.00$) and the smearing was larger $t_I=1.75$ fm. In the present calculations we adopted this procedure, with the JLM(1) interaction, and $N_W=1.00$. The procedure and its parameters determined by this approach were found to give good predictions for the elastic scattering of radioactive nuclei such as ^{7}Be [9] and

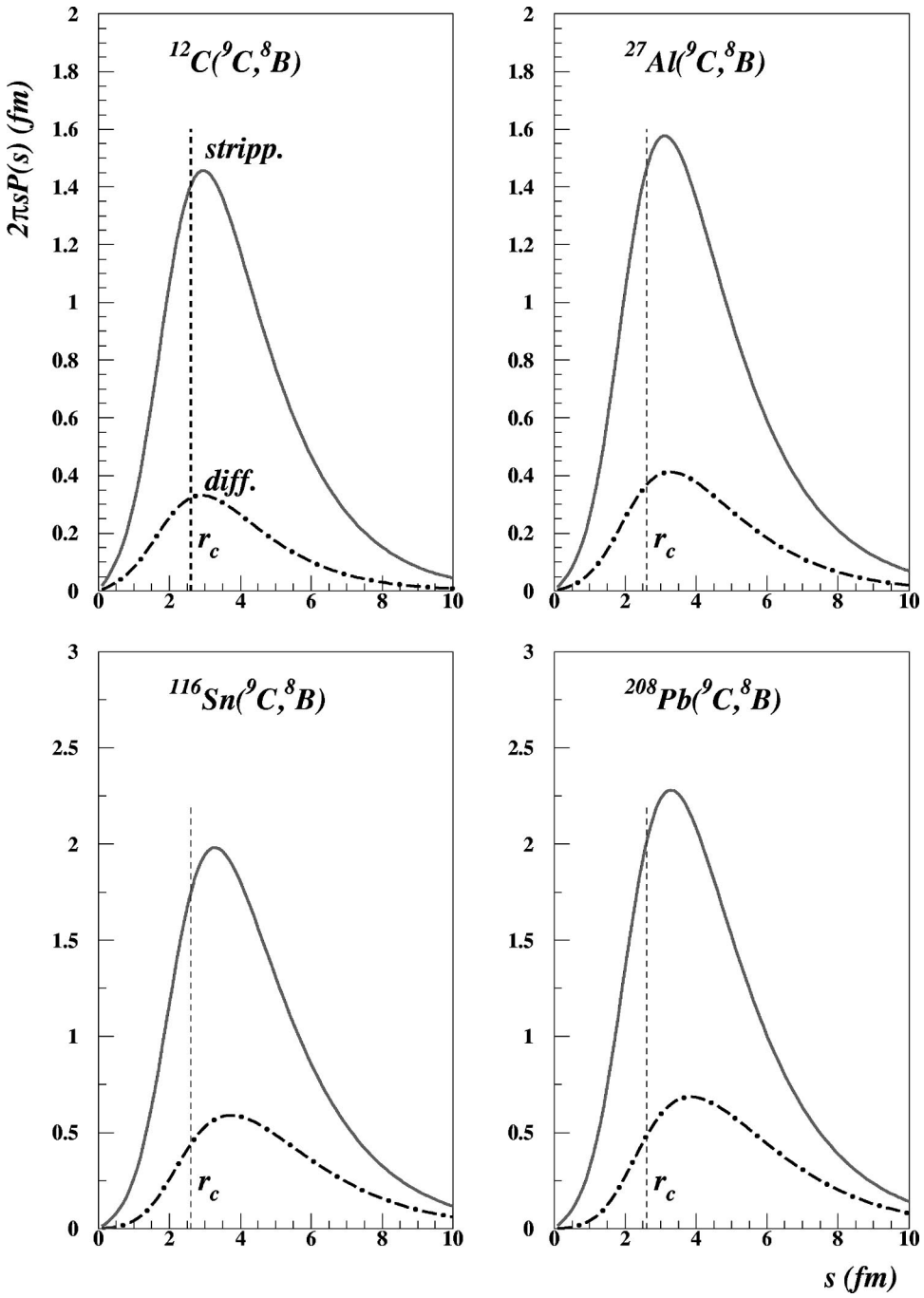

FIG. 2. The stripping and diffraction dissociation contributions to the breakup probability of 285 MeV/nucleon ^{9}C on C, Al, Sn, and Pb targets as a function of the proton impact parameter *s*.

^{11}C [12] at similar energies. We have also checked the procedure on a much wider set of data from the literature at larger energies, and found a similar conclusion for the imaginary part of the potential, while the renormalization of the real part approaches unity around 50 MeV/nucleon. The *S*-matrix calculations that enter the first two terms of Eq. (4) depend primarily on the absorption, and thus on the geometry and strength of the imaginary part of the interaction. The real part of the potential only influences the phases of the scattered waves as the particles go along the classical trajectories and does not affect the total cross section. The Coulomb dissociation term is treated in a perturbative method equivalent to that of Ref. [39], except that radial matrix elements for $E1$ and $E2$ transitions were calculated with realistic Woods-Saxon radial wave functions. Thus both nuclear and Coulomb breakup contributions were calculated in a consistent way.

In order to check that the process was peripheral, the stripping and the diffraction dissociation probabilities were calculated as a function of the parameter *s* (Fig. 1), which is the projection of the proton position vector relative to the core, onto the plane perpendicular to the beam direction. The stripping and the diffraction dissociation probability distributions are shown in Fig. 2. It is clear that for all four targets (the calculations were done for single isotopic targets ^{12}C, ^{27}Al, ^{116}Sn, and ^{208}Pb) the contributions from both terms

peak outside the radius of the assumed ^{8}B core, $R_c = 2.60$ fm [38]. However, the interior does contribute and it should not be discarded. Note that for all four targets the stripping cross section dominates, with the diffraction dissociation part contributing only about 15%. This situation is different from that depicted in Fig. 1 of Ref. [13] where the same two probabilities are shown for the case of ^{8}B breakup on a Si target at 38 MeV/nucleon. In that case the two components of the total cross section have similar magnitudes, with the diffraction dissociation part being slightly larger. This is a well understood bombarding energy effect. High-energy heavy ion interactions are dominated by strong absorption. The ^{8}B calculations are in remarkable agreement with the experimental data that explicitly disentangled the stripping and dissociation reaction mechanisms [23]. The present results are for a much larger energy, and the stripping term (absorption) dominates, as it does for ^{8}B breakup at larger energies. The third term that contributes to the total one-proton-removal cross section, Coulomb dissociation (σ_{Coul}), is the most peripheral due to the long range of the Coulomb forces. It was calculated in its integral form and is not included in Fig. 2. In Fig. 9 of Ref. [40] its radial dependence is shown for situations close to the present one. The present calculations were repeated, changing only the half radius and the diffuseness parameters of the proton binding Woods-Saxon potential that describes the relative motion between the proton and the core on a 20 point grid using $R = 2.20$–2.60 fm in 0.10 fm steps and $a = 0.50$, 0.60, 0.65, and 0.70 fm, but keeping the reaction mechanism parameters unchanged.

From the comparison of the calculations with the experimental cross sections we extracted $C^2_{eff} = C^2_{p_{3/2}} + C^2_{p_{1/2}}$ using Eq. (6). The results are compared in Fig. 3, in order, left to right, for the C, Al, Sn, and Pb targets. The error bars contain the contribution of the experimental errors and of our uncertainties in the calculations, which are described in detail below, added quadratically. The distribution of the four numbers extracted is consistent with the constant value $C^2_{eff} = 1.18 \pm 0.12$ fm^{-1}. The results are also shown in the third column of Table I.

In a second approach, we used the free *NN* *t*-matrix interaction of Franey and Love [41] in a $t\rho\rho$ approximation to obtain the interaction potentials. This is a local representation of the free *NN*-interaction based on phenomenological nucleon-nucleon scattering amplitudes of Arndt *et al.* [42] at several energies between 50 and 1000 MeV. In each spin-isospin channel the interaction is given by a linear combination of Yukawa form factors. The longest range is fixed to be the long range part of the one pion exchange potential, but this part does not survive in the direct term. In the calculation of nucleon-target and projectile-target interactions, the free *NN* *t*-matrix should be renormalized. We used the prescription suggested in [41] employing relativistic kinematics. At intermediate energies one should interpolate in the Franey-Love tabulation. In practice, this procedure is difficult since the number of components varies from energy to energy. At 285 MeV/nucleon we used the parametrization at the nearest energy (300 MeV). Other effects such as Fermi averaging, Pauli blocking and spin-orbit contributions were ignored. Finally, the scattering phase was calculated with Eq. (3) in the lowest order of the eikonal approximation. We have checked however that higher order noneikonal corrections are negligibly small at this energy. The values extracted for C^2_{eff} are similar with those obtained with the JLM interaction and are presented in the fourth column of Table I.

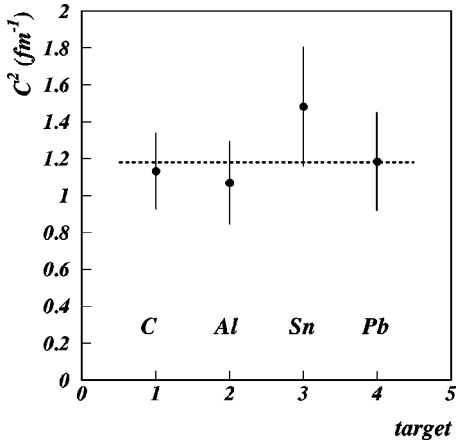

FIG. 3. The asymptotic normalization coefficients determined using the eikonal approach with potentials extracted using JLM interactions. The results are plotted for the C, Al, Sn, and Pb targets (left to right). The uncertainties are a sum in quadrature of the experimental errors and the uncertainties in the calculations.

TABLE I. Summary of the ANC extracted from different ^{9}C breakup reactions and five of the Glauber calculations.

Target	$\sigma(\delta\sigma)$ [mb]	JLM C^2_{eff} [fm^{-1}]	Franey-Love C^2_{eff} [fm^{-1}]	Standard *NN* C^2_{eff} [fm^{-1}]	Ray *NN* C^2_{eff} [fm^{-1}]	Zero-range *NN* C^2_{eff} [fm^{-1}]
C	48(8)	1.132	1.352	1.244	1.304	1.446
Al	55(11)	1.069	1.167	1.077	1.125	1.220
Sn	146(31)	1.482	1.448	1.391	1.438	1.496
Pb	181(40)	1.183	1.140	1.115	1.145	1.172
Average		1.18	1.26	1.19	1.24	1.32

B. Glauber model calculations in the optical limit

At 285 MeV/nucleon, the optical limit of the Glauber model is also applicable. In order to check the cross sections calculated above in the folding model, the *S*-matrix elements were generated in the optical limit which is just the leading term of the cumulant expansion of Glauber's multiple scattering theory:

$$\chi(b)=\frac{1}{2}\sigma_{NN}(i+\alpha_{NN})\int d\vec{b}_1 d\vec{b}_2 \rho_{proj}(b_1) \times \rho_{targ}(b_2)\tilde{v}(\vec{b}+\vec{b}_1-\vec{b}_2), \quad (7)$$

where $\rho_{proj(targ)}(b)$ is the profile density of the projectile (target) obtained from the same Hartree-Fock densities used before:

$$\rho(b)=\int_{-\infty}^{+\infty} dz \rho_{HF}(b,z) \quad (8)$$

(z is the beam direction) and α_{NN} is the ratio of the real to the imaginary nucleon-nucleon forward amplitude. These were interpolated for each isospin state from Table I of Ray [43]. σ_{NN} is the *NN* total cross section at the given energy, taken from the parametrization of Ref. [44]. The integral appearing in Eq. (7) is a projection onto the impact parameter plane of the interaction potential

$$\Omega(R)=\int d\vec{r}_1 d\vec{r}_2 \rho_{proj}(r_1)\rho_{targ}(r_2)\tilde{v}(\vec{r}_1+\vec{R}-\vec{r}_2). \quad (9)$$

Following Ray [43] we identify the Fourier transform of the interaction $\tilde{v}$ with the elementary scattering amplitude:

$$\tilde{v}(q)=-\frac{2\pi\hbar^2}{\mu}f=\frac{\hbar v}{2}\sigma_{NN}(\alpha_{NN}+i)e^{-\beta_{NN}q^2}, \quad (10)$$

where q is the transferred momentum and v is the asymptotic velocity. In practical terms Eq. (9) was solved using a suitably chosen elementary interaction $\tilde{v}$, such as

$$\int d\vec{r} e^{i\vec{q}\vec{r}}\tilde{v}(r)=e^{-\beta q^2} \quad (11)$$

with the solution

$$\tilde{v}(r)=\frac{1}{\pi^{3/2}(4\beta)^{3/2}}e^{-r^2/4\beta}. \quad (12)$$

This was projected onto the impact parameter space and using Eq. (7) the scattering phase was calculated. The amplitudes α_{NN} and the ranges $\mu=\sqrt{4\beta}$ were interpolated from Table I of Ray [43]. In the zero-range approximation, $\mu \to 0$, Eq. (9) is just the overlap volume of the two densities and the scattering phase is determined by the elementary reactions in this volume. The breakup cross section is highly sensitive to the range parameter. To assess this sensitivity we have performed calculations with the ranges prescribed by Ray, with zero range for all interactions and then with an average value of $\mu=1.5$ fm in all pp, nn, and pn channels. This last approach is denoted below as the ''standard'' procedure, as it is widely used to estimate the size of halo nuclei from reaction cross sections [36]. When the incident projectile was a nucleon, then the corresponding profile density was taken as a δ function. We use the charge independence assumption, i.e., $\sigma_{pp}=\sigma_{nn}$, $\sigma_{pn}=\sigma_{np}$, $\alpha_{pp}=\alpha_{nn}$, $\alpha_{pn}=\alpha_{np}$.

One test of the model and of the parameters used to calculate the breakup cross sections, was to see how they reproduce the cross section data for the assumed components of the ^{9}C projectile (p and ^{8}B), separately, on a ^{12}C target (where the nuclear component dominates). We have calculated the reaction cross section and the total cross section for $p+^{12}$C for energies $E=100$ to 1000 MeV, and the reaction cross section for ^{8}B and for ^{9}C in the energy range $E/A=100$ to 1000 MeV/nucleon. The results are compared with experimental data in Fig. 4. The proton reaction cross section data (open circles) in the top panel are taken from the NNDC data base [45] and those for the total cross section (full circles) are from Ref. [46]. The reaction cross section data for ^{8}B shown in the middle panel are from Ref. [15] (filled circles) and Ref. [47] (open circle), while the reaction cross sections for ^{9}C in the lower panel are again from Ref. [15] (filled circle) and from Ref. [48] (open circles), respectively. The calculations shown were done in the zero-range approach, and give a good description of the data over the whole range of energies. Therefore, we have confidence that we can proceed to breakup cross section calculations. We did the calculations with the three range parametrizations described above: Ray, standard, and zero range. For each parametrization, the calculations were repeated on the grid of (R,a) parameters for the proton binding potential, as described above for the JLM potential calculations. Further details of all these calculations will be presented elsewhere [25]. The results are summarized in Table I and are shown in Fig. 5, where they are compared directly with the values already shown in Fig. 3. The error bars are the same as in the preceding figure, and the different points show the values obtained using the three different prescriptions, as explained above. A good consistence can be observed. We underline that the two Glauber approaches are different in essence, and no further parameters were adjusted here. The calculations done in the zero-range approximation gave smaller cross sections (and consequently larger ANCs result) by 5% to 16% (less for Pb, more for ^{12}C target) and we exclude them from the overall average, as the zero-range prescription is not very realistic. A similar check, done with a larger range of the *NN* forces ($\mu=2.5$ fm) shows that the extracted ANCs decrease by 10% to 25%. These also are not included in the average. These two extremes in the range parameter provide a lower and an upper limit on the cross sections. The final average includes the results obtained with four sets of calculations: JLM, Franey-Love, ''standard'' and ''Ray'' *NN* interaction. The weighted average is $C^2_{eff}=1.22\pm0.13$ fm^{-1}, which agrees well with that found from the calculations in the eikonal approach using the JLM interaction. The uncertainty takes into account the experimental uncertainties, and the

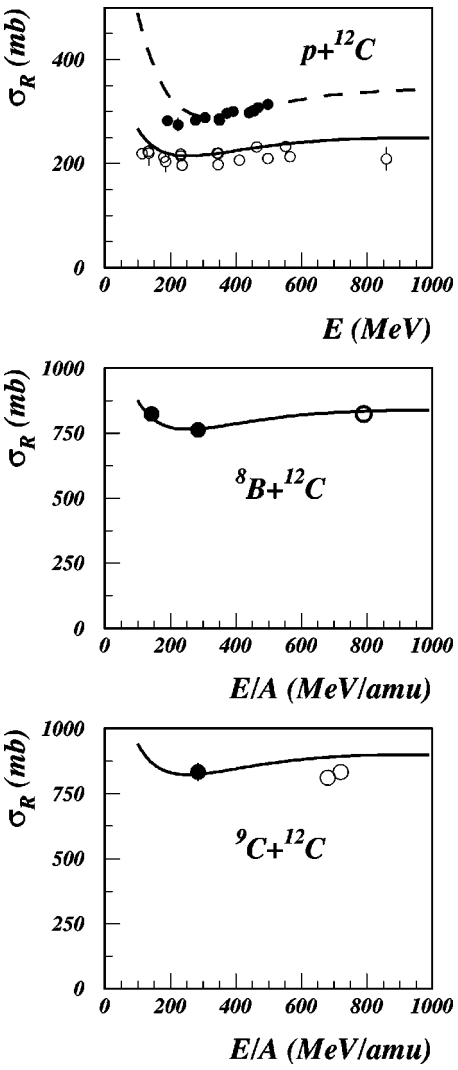

FIG. 4. Comparison of the calculated reaction cross section (full line) and total cross section (dashed line) for $p+{}^{12}\mathrm{C}$ (top panel), and of the reaction cross section of $^{8}\mathrm{B}$ (middle panel) and $^{9}\mathrm{C}$ (bottom panel) on $^{12}\mathrm{C}$ target with experimental data. Data from Refs. [15,45–48] (see text).

uncertainties in the calculations. The ANC values were first averaged for each target, and then an average was calculated for the four targets, using weights given by the quadratically combined experimental and calculational uncertainties. To evaluate the uncertainties for the calculated values we considered independently those arising from the assumed nuclear structure (the geometry of the proton binding potential), as described below, and those from the reaction model. For each target we assumed that the standard deviation of the values obtained from the four different calculations give a fair measure of the reaction model contribution to uncertainty. Averaging first for each type of calculations (as in the last row in Table I), and then for all cases, leads to similar numbers ($C^2_{eff}=1.24\pm0.13$ fm^{-1}), in part because the experimental uncertainties dominate.

A discussion of the validity of the approach used here and of the uncertainties occurring for the particular case of $^{9}\mathrm{C}$ at this energy, *a posteriori*, is in order. The use of such a fragile

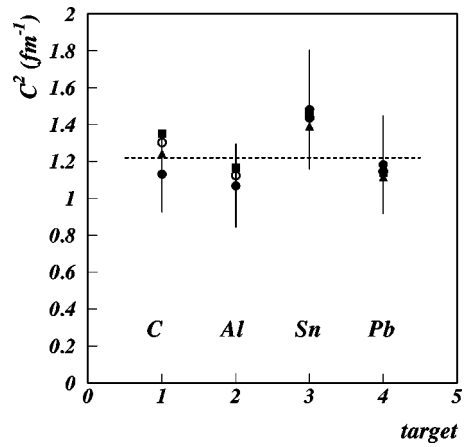

FIG. 5. Same as Fig. 3, but the results of the calculations with Franey-Love (squares), standard *NN* (triangles), and Ray (circles) interactions are added to JLM (filled circles).

nucleus as $^{8}\mathrm{B}$ is as a core can be questioned, and also the high energy (285 MeV/nucleon) may lead to questions about the peripheral nature of the reaction. These questions are supported by the non-negligible contributions of the interior of the $^{9}\mathrm{C}$ nucleus, as shown in Fig. 2. The proton separation energy is not as small here (1.296 MeV) as it was for $^{8}\mathrm{B}$ (0.137 MeV). Using the procedure of Ref. [38], and the ANC extracted we find the rms radius of the last proton in $^{9}\mathrm{C}$ to be $\langle r^2\rangle^{1/2}=3.02$ fm, considerably smaller than that found for $^{8}\mathrm{B}$: $\langle r^2\rangle^{1/2}=3.97$ fm. This, and the large separation energy, reflects in a less sharp definition of the extracted ANC. In a figure equivalent to Fig. 2 of Ref. [13], the ANC line has a larger slope, pointing towards the conclusion that there is a residual dependence on the geometry of the proton binding Woods-Saxon potential chosen. This contribution to the uncertainty varies between 7.8% and 4.6% for the targets between C and Pb, and is clearly smaller than the experimental uncertainties, and was considered in the uncertainties plotted in Figs. 3 and 5. No new parameters were adjusted in the present calculations. However some parameters were extracted before, with corresponding uncertainties. For the case of the extended Glauber model calculations with the JLM interaction, these parameters are the renormalization (N_R, N_W) and the finite range (t_R, t_I) parameters of the real and imaginary parts of the nucleus-nucleus potential and have uncertainties. To see how these propagate to calculated breakup cross sections, we repeated the calculations varying individually each parameter. We discussed above that the real potential does not influence the total cross section. Thus only the influence of t_I and N_W was determined. We found the relative variation of the extracted ANC $\delta C^2_{eff}/C^2_{eff}$ to be from $\pm6.4\%$ on the C and Al targets, down to $\pm3.3\%$ on the Pb target (the relative contribution of the nuclear breakup decreases as the charge of the target increases), when the renormalization coefficient N_W varies in the range found in Ref. [34] $N_W=1.00\pm0.09$. Similarly, a change of 4.7% to 3.0% was found for a variation of 10% around the central value of the smearing range $t_I=1.75$ fm. Combining the two in quadrature we obtain an 8% uncertainty, which is smaller than the experimental uncertainties are, and similar to the

uncertainties from the choice of the model. For the calculations in the optical limit, the differences between the three approaches used give an assessment of their overall uncertainty. The maximum deviation around the average is less than 7–8 % in each case. Our present model does not consider two-step processes such as $^{9}\mathrm{C}\rightarrow{}^{8}\mathrm{B}+p\rightarrow{}^{7}\mathrm{Be}+p+p$ and we cannot therefore directly assess their importance. However, a recent paper [49] compares Glauber model calculations using a three-body projectile model with those using a two-body projectile (as used in our calculations) and finds the dynamical correlations to have a small influence (less than 10%) on the calculated one-neutron-removal cross section for the (^{12}Be, ^{11}Be) and (^{16}C, ^{15}C) reactions, a finding that supports the spectator assumption even when the spectator itself is a loosely bound system, as in the case of ^{9} C. The situations considered there are similar to the present one, as ^{11} Be (assumed core for ^{12}Be) and ^{15}C (core for ^{16}C) are halo nuclei of an even larger extent than ^{8}B (core for ^{9}C) and, therefore, expect the effect of two-step processes to be even smaller for our case.

In a recent publication [11], the ANC for $^{9}\mathrm{C}\rightarrow{}^{8}\mathrm{B}+p$ was found using the proton transfer reaction $d(^{8}\mathrm{B},^{9}\mathrm{C})n$ at 14.4 MeV/nucleon incident energy. The experimental statistics were rather poor, according to their Fig. 1, and the authors present the results of a range of DWBA calculations, with different optical potentials from literature. They report an effective ANC that ranges from 0.97 to 1.42 fm^{-1}, with an average that we found to be $\langle C^{2}_{eff}\rangle=1.18$ fm^{-1}. From their assessment of the final uncertainty we figure $\delta C^{2}_{eff}=0.34$ fm^{-1}. This uncertainty is large (30%), and (d,n) reactions have been criticized before [50] for not being good peripheral reactions, inadequate for the determination of the ANC. However, their values (and particularly the average) are very close to those extracted by us from different experimental data and using a different reaction mechanism.

III. THE ASTROPHYSICAL FACTOR S_{18}

Since the $^{8}\mathrm{B}(p,\gamma)^{9}\mathrm{C}$ capture process at astrophysical energies is a peripheral process, the absolute normalization of its astrophysical S_{18} factor is entirely defined by the ANC for $^{8}\mathrm{B}+p\rightarrow{}^{9}\mathrm{C}$. To calculate the astrophysical S factor we used the potential model, as described in Ref. [51]. Electric dipole and quadrupole transitions were included for the final channel, with $E1$ giving the largest contribution, and practically all waves were considered in the entrance channel (but the s-wave dominates the major $E1$ term and the d-wave contributes only a few percent). The calculations were done with a single proton $1p_{3/2}$ wave function normalized to unity and having the asymptotic normalization coefficient b_{p}. Then the result was scaled by C^{2}_{eff}/b^{2}_{p} (such a procedure avoids any complications that might appear when a Whittaker function normalized by C_{eff} is used over the whole integration range). The calculations were done for the proton energy range $E_{cm}=0-0.8$ MeV. The contribution of the resonant state at $E_{res}=922$ keV with known width $\Gamma=100$ keV was found to be unimportant here, because is rather far away and most likely its spin is $J^{\pi}=1/2^{-}$ and thus it is forbidden by selection rules to contribute to the major term. A very weak dependence on energy is observed: $S(E)=45.8-15.1E+7.34E^{2}$ (E in MeV), less than 15% decrease on the whole range.

Therefore, we find a value $S_{18}(0)=46\pm6$ eV b. This value is in agreement with the value $S_{18}(0)=45\pm13$ eV b reported in Ref. [11], but disagrees with those previously obtained from various calculations. This radiative capture process was investigated in a microscopic cluster model using the generator coordinate method with two different potentials (Volkov $V2$ and Minnesota) in Ref. [52]. The author obtained for $S_{18}(0)$ values around 80 and 90 eV b, respectively, therefore 80–100 % larger than our value. Earlier, Ref. [2] used a single particle model to estimate the S-factor and obtained a much larger value (210 eV b), almost certainly because of the too large spectroscopic factor $C^{2}S=2.5$ that they use. A short communication by Timofeyuk [53] reported a value $S_{18}(0)=53$ eV b from microscopic calculations using the $M3Y$ nucleon-nucleon interaction, via an estimate of the ANC and of the equivalent vertex constant, but without giving too many details about the calculations. This last calculation is closer to the experimental value determined here. Significant disagreement between the astrophysical factors obtained in Ref. [52] and to a certain extent in Ref. [53] using different potentials (although in slightly different microscopic approaches) demonstrates the sensitivity of the calculated ANCs to the effective NN-potentials adopted for the nuclear structure calculations. Such sensitivity has been observed before for the $1p$-shell nuclei in Ref. [54]. Later the generator coordinate method (GCM) calculations with Volkov potentials [55] led to an ANC for the system $^{7}\mathrm{Be}+p\rightarrow{}^{8}\mathrm{B}$ about 70% higher than the ANC determined experimentally from proton transfer reactions [9] and from the breakup reaction of ^{8}B [13]. The most instructive dependence of the microscopically calculated ANCs on the adopted effective NN-potential has been demonstrated by Baye and Timofeyuk [Ref. [56]]. The authors investigated the sensitivity of the nuclear vertex constant (which is the ANC up to a trivial kinematical factor) for the system $^{16}\mathrm{O}+n\rightarrow{}^{17}\mathrm{O}$ calculated in the microscopic GCM for ten different effective NN potentials. All the adopted potentials, among which were six Volkov potentials, HNY, Minnesota, and Gogny potentials, significantly overestimated the experimental nuclear vertex constant, as appears also to be the case here. For example, $V2$ (Volkov 2) potential overestimates the ANC by 50%. Hence the overestimation of the microscopically calculated ANCs has a long history and the present result for $^{8}\mathrm{B}+p\rightarrow{}^{9}\mathrm{C}$ once more seems to confirm that.

Using the astrophysical S factor obtained above from the experimental ANC for the energy region $E_{\mathrm{c.m.}}=0-0.8$ MeV we evaluated the reaction rate shown in Fig. 6 for the temperature range $T_{9}=0-1$, which covers the relevant temperature range for explosive hydrogen burning in supernovae [2]. Using the expansion for the reaction rate in powers of T_{9} [1] (for the case of slowly varying astrophysical S factors):

$$R=N_{A}\langle\sigma v\rangle=T_{9}^{-2/3}\exp\left(-\frac{B}{T_{9}^{1/3}}\right)(A_{0}+A_{1}T_{9}^{1/3}+A_{2}T_{9}^{2/3})\times(\mathrm{cm}^{3}/\mathrm{s\,mol}^{-1}), \quad (13)$$

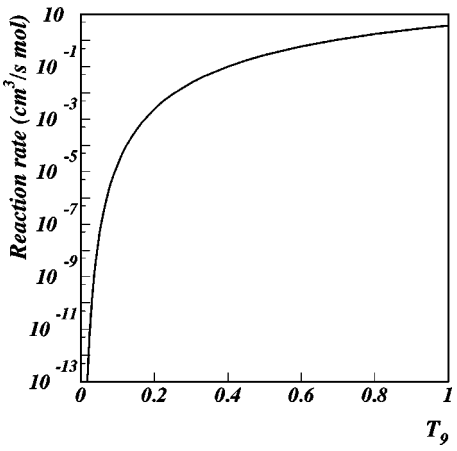

FIG. 6. The estimated reaction rate for the temperature range $T_9=0-1$.

where N_A is Avogadro's number, T_9 is the temperature in 10^9 K, and

$$B=3\left[\left(\frac{\pi e^2 Z_1 Z_2}{\hbar}\right)^2 \frac{\mu}{2k}\right]^{1/3}$$
$$=4.249[\mu[\mathrm{amu}]Z_1^2 Z_2^2]^{1/3} \quad (10^9 K)^{-1/3}. \qquad (14)$$

We found that we can reproduce the calculated temperature variation with the constants: $B=11.945$ (not fitted), $A_0=6.64\times10^5$, $A_1=8.50\times10^4$ and $A_2=-2.41\times10^5$. The formula fits the integrated reaction rates with an accuracy of 0.5% over the range $T_9=0-1$.

IV. CONCLUSIONS

We have used existing experimental cross section data for the breakup of the unstable nucleus ^{9}C at 285 MeV/nucleon on four different targets [15] to determine the ANC of the radial overlap integral of the last proton orbiting its core by comparing them with Glauber model calculations in the eikonal approximation. Two different approaches were used to generate *S*-matrix elements. In the first approach, both *G*-matrix and *t*-matrix effective interactions were folded with Hartree-Fock single particle densities in order to obtain the interaction potentials. In the second approach, the optical limit of Glauber's multiple scattering theory was used with three prescriptions for the elementary amplitudes. All calculations gave consistent results. There were no new parameters that were adjusted in the present calculations. We found the ANC for the virtual decay $^9\mathrm{C}\rightarrow{}^8\mathrm{B}+p$, and then the astrophysical factor S_{18} for the radiative proton capture reaction $^8\mathrm{B}(p,\gamma)^9\mathrm{C}$. This reaction gives a possible path to the hot *pp* chain *pp-IV* at high temperatures and away from it toward a rapid alpha process *rap I* at high temperatures and densities [2].

Moreover, we show here a case where the indirect determination of nuclear astrophysical information from the breakup of unstable nuclei at intermediate energies proposed by us earlier for ^{8}B, shows its usefulness. The method we use was tested so far only for the case of ^{8}B [13] for which an independent knowledge of the ANC exists, and this is a second case we propose. We also note that the breakup cross sections are somewhat larger than those for the transfer reactions (around 100 mb, compared with a few mb for proton transfer) due to the fact that essentially the whole range of radii from about the grazing radius to infinity participates, whereas for transfer only a limited region around the grazing radius is involved.

Better experimental data, including detailed momentum distributions and eventually disentangling the contribution of the stripping and diffraction dissociation processes would provide additional information to check the reliability of the models used. Also more breakup data in the same region of nuclei would provide valuable information to check the parameters and procedures used in these calculations and increase their overall reliability.

ACKNOWLEDGMENTS

One of us (F.C.) acknowledges the support of IN2P3 for a stay at Laboratoire de Physique Corpusculaire in Caen, during which part of this work was completed. The work was supported by the U.S. Department of Energy under Grant No. DE-FG03-93ER40773 and by the Romanian Ministry for Research and Education under Contract No. 555/2000.

[1] C.E. Rolfs and W.S. Rodney, *Cauldrons in Cosmos* (University of Chicago Press, Chicago, 1988).
[2] M. Wiescher, J. Görres, S. Graff, L. Buchman, and F.-K. Thieleman, Astrophys. J. **343**, 352 (1989).
[3] A.E. Champagne and M. Wiescher, Annu. Rev. Nucl. Part. Sci. **42**, 39 (1992).
[4] F. Kaeppeller, F.-K. Thielemann, and M. Wiescher, Annu. Rev. Nucl. Part. Sci. **48**, 175 (1998).
[5] C. Rolfs, Nucl. Phys. **A217**, 29 (1973).
[6] A.M. Mukhamedzhanov and N.K. Timofeyuk, Pis'ma Zh. Eksp. Teor. Fiz. **51**, 247 (1990) [JETP Lett. **51**, 282 (1990)].
[7] H.M. Xu, C.A. Gagliardi, R.E. Tribble, A.M. Mukhamedzhanov, and N.K. Timofeyuk, Phys. Rev. Lett. **73**, 2027 (1994).
[8] A. Azhari, V. Burjan, F. Carstoiu, H. Dejbakhsh, C.A. Gagliardi, V. Kroha, A.M. Mukhamedzhanov, L. Trache, and R.E. Tribble, Phys. Rev. Lett. **82**, 3960 (1999); Phys. Rev. C **60**, 055803 (1999).
[9] A. Azhari, V. Burjan, F. Carstoiu, C.A. Gagliardi, V. Kroha, A.M. Mukhamedzhanov, F.M. Nunes, X. Tang, L. Trache, and R.E. Tribble, Phys. Rev. C **63**, 055803 (2001).
[10] W. Liu *et al.*, Phys. Rev. Lett. **77**, 611 (1996).
[11] D. Beaumel *et al.*, Phys. Lett. B **514**, 226 (2001).
[12] X.D. Tang, Ph.D. thesis, Texas A&M University, 2002.
[13] L. Trache, F. Carstoiu, C.A. Gagliardi, and R.E. Tribble, Phys. Rev. Lett. **87**, 271102 (2001).
[14] R.J. Glauber, in *Lectures in Theoretical Physics*, edited by W.E. Brittin and L.G. Dunham (Interscience, New York, 1959).

[15] B. Blank *et al.*, Nucl. Phys. **A624**, 242 (1997).
[16] I. Tanihata, J. Phys. G **22**, 157 (1996).
[17] P.G. Hansen and B.M. Sherrill, Nucl. Phys. **A693**, 133 (2001).
[18] D. Cortina-Gil *et al.*, Phys. Lett. B **529**, 36 (2002).
[19] J.A. Tostevin, Nucl. Phys. **A682**, 320c (2001).
[20] L. Trache, C.A. Gagliardi, A.M. Mukhamedzhanov, R.E. Tribble, F. Carstoiu, and E. Sauvan, Bull. Am. Phys. Soc. **46(7)**, 64 (2001).
[21] V.R. Pandharipande, I. Sick, and P.K.A. de Witt Huberts, Rev. Mod. Phys. **69**, 981 (1997), and references therein.
[22] B.A. Brown, P.G. Hansen, B.M. Sherrill, and J.A. Tostevin, Phys. Rev. C **65**, 061601(R) (2002).
[23] F. Negoita *et al.*, Phys. Rev. C **54**, 1787 (1996).
[24] E. Sauvan *et al.*, Phys. Lett. B **491**, 1 (2000).
[25] F. Carstoiu *et al.* (unpublished).
[26] G. Bertsch, H. Esbensen, and A. Sustich, Phys. Rev. C **42**, 758 (1990).
[27] H. Esbensen and G.F. Bertsch, Phys. Rev. C **64**, 014608 (2001).
[28] G. R. Satchler, *Direct Nuclear Reactions* (Oxford University Press, New York, 1983).
[29] L.D. Blokhintsev, I. Borbely, and E.I. Dolinskii, Fiz. Elem. Chastits At. **8**, 1189 (1977) [Sov. J. Part. Nucl. **8**, 485 (1977)].
[30] S.J. Wallace, Phys. Rev. C **8**, 2043 (1973).
[31] L. Trache *et al.*, Phys. Rev. C **54**, 2361 (1996).
[32] J.P. Jeukenne, A. Lejeune, and C. Mahaux, Phys. Rev. C **16**, 80 (1977).
[33] E. Bauge, J.P. Delaroche, and M. Girod, Phys. Rev. C **58**, 1118 (1998).
[34] L. Trache, A. Azhari, H.L. Clark, C.A. Gagliardi, Y.-W. Lui, A.M. Mukhamedzhanov, R.E. Tribble, and F. Carstoiu, Phys. Rev. C **61**, 024612 (2000).
[35] M. Beiner and R.J. Lombard, Ann. Phys. (N.Y.) **86**, 262 (1974); F. Carstoiu and R.J. Lombard, *ibid.* **217**, 279 (1992).
[36] G.F. Bertsch, B.A. Brown, and H. Sagawa, Phys. Rev. C **39**, 1154 (2001).
[37] B.A. Brown, S. Typel, and W.A. Richter, Phys. Rev. C **65**, 014612 (2001).
[38] F. Carstoiu, L. Trache, C.A. Gagliardi, R.E. Tribble, and A.M. Mukhamedzhanov, Phys. Rev. C **63**, 054310 (2001).
[39] C. Bertulani and G. Baur, Nucl. Phys. **A480**, 615 (1988).
[40] H. Esbensen and K. Hencken, Phys. Rev. C **61**, 054606 (2000).
[41] W.G. Love and M.A. Franey, Phys. Rev. C **24**, 1073 (1981); **31**, 488 (1985).
[42] R.A. Arndt, R.H. Hackman, and L.D. Roper, Phys. Rev. C **9**, 555 (1974); **15**, 1002 (1977).
[43] L. Ray, Phys. Rev. C **20**, 1857 (1979).
[44] S. John, L.W. Townsend, J.W. Wilson, and R.K. Tripathi, Phys. Rev. C **48**, 766 (1993).
[45] Data retrieved from the National Nuclear Data Center, Brookhaven National Laboratory Online Data Service.
[46] P. Schwaller, M. Pepin, B. Favier, C. Richard-Serre, D.F. Measday, and P.U. Renberg, Nucl. Phys. **A316**, 317 (1979).
[47] I. Tanihata, T. Kobayashi, O. Yamakawa, S. Shimoura, K. Euni, K. Sugimoto, N. Takahashi, T. Shimoda, and H. Sato, Phys. Lett. B **206**, 592 (1988).
[48] A. Ozawa, I. Tanihata, T. Kobayashi, Y. Sugahara, O. Yamahawa, K. Omata, K. Sugimoto, D. Olson, W. Christie, and H. Wieman, Nucl. Phys. **A608**, 63 (1996).
[49] J.S. Al-Khalili, Nucl. Phys. **A689**, 551c (2001).
[50] C.A. Gagliardi, A.M. Mukhamedzhanov, R.E. Tribble, and H.M. Xu, Phys. Rev. Lett. **80**, 421 (1998).
[51] R.F. Christy and I. Duck, Nucl. Phys. **24**, 89 (1961).
[52] P. Descouvemont, Nucl. Phys. **A646**, 261 (1999).
[53] N. Timofeyuk, in *International School-Seminar on Heavy Ion Physics*, edited by Yu. Ts. Oganessian *et al.* (Dubna, Russia, 1993), Vol. 2, p. 534.
[54] A.M. Mukhamedzhanov and N. Timofeyuk, Yad. Fiz. **51**, 679 (1990) [Sov. J. Nucl. Phys. **51**, 431 (1990)].
[55] P. Descouvemont and D. Baye, Nucl. Phys. **A567**, 341 (1994).
[56] D. Baye and N.K. Timofeyuk, Phys. Lett. B **293**, 13 (1992).